REPORT

Spermatogenesis 1:2, 123-136; April/May/June 2011; © 2011 Landes Bioscience

Actin-binding protein drebrin E is involved in junction dynamics during spermatogenesis

Michelle W.M. Li,[1,†] Xiang Xiao,[1,†] Dolores D. Mruk,[1] Yee-ling Lam,[1] Will M. Lee,[2] Wing-yee Lui,[2] Michele Bonanomi,[3] Bruno Silvestrini[3] and C. Yan Cheng[1,*]

[1]Center for Biomedical Research; The Population Council; New York, NY USA; [2]School of Biological Sciences; The University of Hong Kong; Hong Kong, China; [3]S.B.M. Srl; Rome, Italy

[†]These authors contribute equally to this work.

Key words: testis, spermatogenesis, blood-testis barrier, drebrin, drebrin E, actin-binding protein, apical ectoplasmic specialization

The actin-based cytoskeleton plays a critical role in the seminiferous epithelium during spermatogenesis by conferring cell shape, adhesion, structural support and cell polarity to both Sertoli and developing germ cells, which are essential for spermatogonial stem cell renewal, maintenance of the stem cell niche, cell cycle progression, mitosis, meiosis, spermiogenesis and spermiation. However, few functional studies are found in the literature, which explore the functional significance of actin dynamics in these events. This by and large is due to a lack of information on the proteins that regulate actin dynamics. Herein, we report drebrin E is an integrated component of the apical ectoplasmic specialization (apical ES) and the basal ES at the blood-testis barrier (BTB) in the seminiferous epithelium of the adult rat testis. Using immunohistochemistry and dual-labeled immunofluorescence analysis, drebrin E was found to display a stage-specific localization at the apical ES, as well as at the basal ES at the BTB during the seminiferous epithelial cycle of spermatogenesis. Drebrin E was first detected in stage V tubules at the basal ES with the highest expression at the BTB at stages V and VI, but it diminished considerably by stages VII and VIII and was almost non-detectable until stage IV. At the apical ES, drebrin E was also first detected at stage V, surrounding the entire head of the elongating spermatid, but by stage VI its localization had "shifted" to localize most intensely and almost exclusively to the concave side of the spermatid head. In stage VII tubules, drebrin E co-localized with actin, as well as with two other actin regulatory proteins Eps8 (epidermal growth factor receptor pathway substrate 8, an actin capping and bundling protein) and Arp3 (actin-related protein 3, a component of the Arp2/3 complex known to regulate actin nucleation and branching). The localization of drebrin E at the apical ES was compromised following treatment of rats with adjudin, which is known to exert its destructive effects primarily at the apical ES by inducing premature loss of elongating/elongated spermatids from the epithelium, mimicking "spermiation." Instead of being restricted to the concave side of spermatid heads, drebrin E was found to be mis-localized in the seminiferous epithelium of adjudin-treated rats; it was also present on the convex side of elongating spermatids, but these cells were mis-oriented so that their heads no longer pointed toward the basement membrane. The expression of drebrin E by Sertoli cells was also found to be modulated by TGFβ3 and TNFα. Since Arp3, but not Eps8, was found to bind drebrin E; and cytokines were also shown to affect the cellular distribution of drebrin E and enhance the interaction between drebrin E and Arp3, these findings illustrate that cytokines may regulate BTB dynamics during the epithelial cycle by recruiting drebrin E and Arp3 to the BTB microenvironment to induce changes in the configuration of actin filament bundles at the basal ES. In summary, these findings illustrate drebrin E is working in concert with Arp3 to regulate actin filament bundles at both the apical and the basal ES in the testis, conferring adhesion and cell polarity at both sites during spermatogenesis.

Introduction

One of the primary functions of the mammalian testis is to produce spermatozoa via spermatogenesis, which takes place in the seminiferous epithelium of seminiferous tubules composed of Sertoli cells and developing germ cells, and is under the influence of LH, FSH, testosterone and estrogen.[1-10] In the seminiferous tubules, a unique ultrastructure known as the blood-testis barrier (BTB), which is created by coexisting tight junctions (TJ), basal ectoplasmic specializations (basal ES), desmosomes and gap junctions (GJs) near the basement membrane, physically divides the seminiferous epithelium into the basal and the apical (or adluminal) compartment.[1,2,11] Besides (1) the renewal of spermatogonia via mitosis, (2) the proliferation and differentiation of type A spermatogonia and (3) their transformation into type B spermatogonia and preleptotene spermatocytes that take place in the basal compartment of the seminiferous epithelium, the cellular and molecular events of (4) meiosis I and II, (5) spermiogenesis and (6) spermiation all take place behind the BTB in the adluminal compartment. Thus, germ cell-specific antigens

*Correspondence to: C. Yan Cheng; Email: Y-cheng@popcbr.rockefeller.edu
Submitted: 04/11/11; Revised: 05/06/11; Accepted: 05/07/11
DOI: 10.4161/spmg.1.2.16393

arising during meiosis, spermiogenesis and spermiation can be sequestered from the host's immune system to avoid the production of anti-sperm antibodies.[2,12] It is known that preleptotene/leptotene spermatocytes connected by cytoplasmic bridges to form clones are in transit at the BTB at stage VIII of the seminiferous epithelial cycle and enter the apical compartment while differentiating into zygotene spermatocytes to prepare for diakinesis, to be followed by meiosis I and II. During spermiogenesis, developing spermatids continue their journey across the remaining seminiferous epithelium by first moving upward and toward (at stages I–III) the tubule lumen, and then back downward and toward the BTB (at stages IV and V) near the basement membrane, before moving toward the adluminal edge of tubule lumen again (at stages VI and VII) prior to their release at stage VIII (i.e., spermiation).[13-15] Thus, it is conceivable that there is extensive junction restructuring taking place at the cell-cell interface, involving constant remodeling of the cytoskeleton to facilitate these events.[16-18] Interestingly, the basal ES which is found at the Sertoli-Sertoli cell interface at the site of the BTB and the apical ES which is restricted to the Sertoli cell-spermatid (from step 8–19 spermatids in rats) interface, share similar ultrastructural features, that is, actin filament bundles sandwiched in between cisternae of endoplasmic reticulum and the apposing Sertoli cell or Sertoli cell-spermatid plasma membranes.[1,16,18] Earlier studies have shown that these actin filament (F-actin) bundles are maintained by actin bundling and capping proteins [e.g., epidermal growth factor receptor pathway substrate 8 (Eps8)],[19] and actin nucleation proteins [e.g., actin-related protein 3 (Arp3) of the Arp2/3 complex].[20] Interestingly, these actin-associated proteins are also known to participate in endocytic vesicle-mediated trafficking at the cell-cell interface to "stabilize" or "de-stabilize" cell adhesion protein complexes, facilitating spermatid movement.[15,16]

In this study, we have examined the potential role of an actin binding protein (also known as microfilament-associated protein), drebrin (developmentally regulated brain protein),[21,22] in junction dynamics during spermatogenesis. To date, three isoforms of drebrin have been identified, which are members of the ADF-H (actin depolymerizing factor homology) domain family of actin-binding proteins.[23] They were initially identified in chicken as neuronal drebrin isoforms A (adult) and E1 and E2 (embryonic).[24,25] In rats, two isoforms of drebrin are presently known to exist, which include the adult neuronal cell-specific drebrin A restricted to brain and the embryonic isoform drebrin E, which is a splice variant of drebrin A;[26] whereas drebrins 1a and 1b and drebrins A, A2 and E2 are found in humans and mice, respectively.[25] While drebrin A is adult brain-specific, drebrin E has been detected in multiple organs including the stomach, kidney and testis, but not in cardiac or skeletal muscles.[27,28] Despite the presence of an ADF-H domain in drebrin and the fact that it binds F-actin with high affinity in vitro, drebrin has not been found to possess any F-actin severing, bundling, capping and/or nucleating activity.[21,29-31] However, drebrin can compete with α-actinin, fascin and tropomyosin for binding to F-actin,[21,24,27] and drebrin E was shown to inhibit the actin-crosslinking, as well as the actin-binding activity, of α-actinin.[24] Thus, even though drebrin does not possess any intrinsic activity to regulate actin dynamics per se, it appears to regulate actin filament bundles at the ES by interacting (or competing) with other F-actin regulatory proteins that are either directly or indirectly involved in actin polymerization/depolymerization. For instance, in neuronal cells, drebrin A has been correlated with changes in cell shape and actin plasticity, and thus has been implicated in regulation of actin dynamics.[26,32] Herein, we report findings on the role of drebrin E in actin dynamics in the testis using different in vivo and in vitro study models. We also demonstrate herein that Arp3 is a binding partner of drebrin E in the testis and that the interaction of Arp3 with drebrin E is under the influence of cytokines (e.g., TNFα, TGFβ3) which, in turn, affect the actin filament network in Sertoli cells at the BTB. This is the subject of the present report.

Results

Stage-specific expression and localization of drebrin E at the BTB and apical ES during the seminiferous epithelial cycle of spermatogenesis. While drebrin A and E isoforms were both detected in the brain by immunoblotting, only drebrin E was found in the testis by immunoblot analysis (**Fig. 1A**). Drebrin E was also preferentially expressed by Sertoli cells vs. germ cells (**Fig. 1**). The specificity of this anti-drebrin antibody (see **Table 1**) was confirmed by immunoblotting using Sertoli cell lysates as shown in **Figure 1B**. This antibody was subsequently used for immunohistochemistry (**Fig. 1C**) and immunofluorescence microscopy (**Fig. 1D**), illustrating the staining shown in **Figure 1C and D** was specific for drebrin E. Besides its cell type-dependent expression in the testis, its localization in the seminiferous epithelium was dependent on the stage of the epithelial cycle when immunoreactive drebrin E in the epithelium was visualized (**Fig. 1C and D**). Immunoreactive drebrin E was detected at the BTB and at the apical ES in the seminiferous epithelium in adult rat testes. Drebrin E was found at the apical ES surrounding the entire head of elongating spermatids beginning at stages IV and V (**Fig. 1C and D**). It localized more intensely to the concave side of the spermatid head at stage VI and became highly expressed at this same site at stage VII, but diminished considerably at stage VIII (**Fig. 1C and D**). The concave side of the spermatid head is the site of the apical ES where extensive endocytic vesicle-mediated protein trafficking occurs beginning at late stage VII to allow the apical ES to undergo disruption, thereby preparing spermatids for their eventual release at spermiation.[1,13,33] Interestingly, drebrin E was also highly expressed at the BTB at stages IV and V of the epithelial cycle by immunohistochemistry (**Fig. 1C**) or immunofluorescence microscopy (**Fig. 1D**), but it diminished considerably at stages VII–VIII, apparently to prepare the BTB for its restructuring at stage VIII to facilitate the transit of preleptotene spermatocytes across the barrier. Interestingly, the expression of drebrin E was even lower at stages XII–XIV. In short, at stage VIII, when spermiation and BTB restructuring occur, drebrin E expression was considerably reduced at both sites, coinciding with the disruption of actin filament bundles at the basal and apical ES.

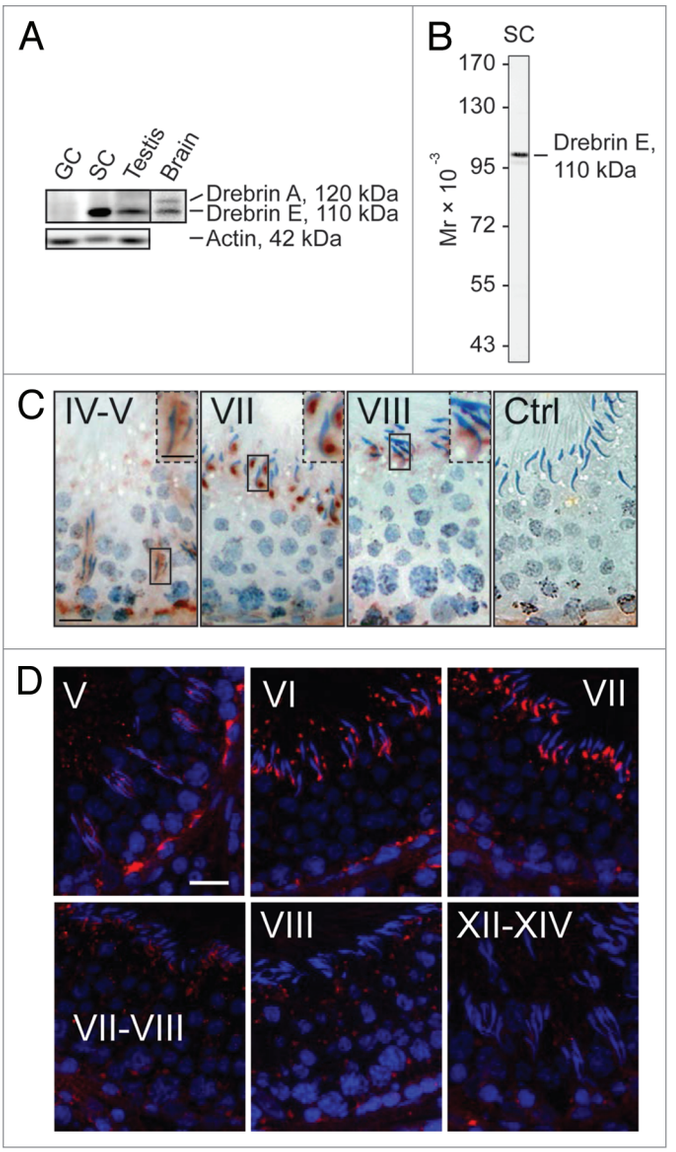

Figure 1. Drebrin E is expressed stage-specifically in the seminiferous epithelium of adult rat testes. (A) Using immunoblot analysis with ~50 μg total protein per sample, only the drebrin E isoform was found to be expressed in the testis while both drebrin A and E isoforms were detected in brain lysate. Drebrin E was predominantly expressed by Sertoli cells (SC) in the seminiferous tubule and virtually no drebrin E was found in total germ cells (GC) isolated from adult rat testes. Actin served as the protein loading control. (B) The specificity of the anti-drebrin E antibody was illustrated by immunoblotting using lysates of Sertoli cells (~50 μg protein) since only a prominent immunoreactive band corresponding to the apparent Mr of drebrin E at 110 kDa was detected. These results also support the staining shown in (C and D) was specific for drebrin E. A study using immunohistochemistry (C) and immunofluorescence microscopy (D; drebrin E, red fluorescence; cell nuclei were visualized by DAPI in blue, 4′,6-diamidino-2-phenylindole, staining) showed that drebrin E localized near the basement membrane in the basal compartment, consistent with its localization at the blood-testis barrier (BTB), and drebrin E also localized at the apical ectoplasmic specialization (apical ES). The expression of drebrin E at the BTB is most prominent at stage V of the seminiferous cycle using both staining techniques (C and D), which diminished gradually thereafter and was almost non-visible at the BTB by stages VIII–XIV. In (C), the boxed areas enclosed by a "solid-line" rectangle notes an area of the epithelium that was magnified; this is shown in the same micrograph but enclosed within a "broken-line" rectangle. Ctrl illustrates sections that were stained with normal rabbit IgG which was substituted in place of the anti-drebrin E antibody, confirming the reddish-brown immunoreactive drebrin E shown in (C) was specific for drebrin E. Drebrin E was localized at the apical ES, surrounding the entire head of the elongating spermatid at stages IV and V (C). However, the localization of drebrin E shifted and localized predominantly to the concave side of the head of elongating/elongated spermatids at stage VII (see also the magnified images in C), but its level was drastically reduced at stage VIII and these observations were consistent using either immunohistochemistry (C) or immunofluorescence microscopy (D). Roman numerals denote stages of the seminiferous epithelial cycle. Bar = 50 μm in the first micrograph in (C and D), which also applies to the other micrographs; bar = 25 μm in the inset in the first micrograph in (C), which also applies to the other insets in (C). These micrographs are representative results from a single set of experiments, which were repeated at least 3 times using different sets of sections from different rats and similar results were obtained.

Co-localization of drebrin E with the F-actin network and its regulators. Since drebrin E is an actin binding protein,[22,26] its localization was compared with that of F-actin and two actin regulators, Eps8 (an actin bundling and capping protein) and Arp3 (an actin nucleation regulator) (**Fig. 2**). At stage V of the seminiferous epithelial cycle, drebrin E expression in the seminiferous epithelium near the basement membrane, consistent with its localization at the BTB, was relatively high (see also **Fig. 1C and D**). Drebrin E was found to co-localize with F-actin in the epithelium near the basement membrane, consistent with its localization at the site of the BTB (**Fig. 2**). However, drebrin E also co-localized with F-actin at the apical ES, surrounding almost the entire head of elongating spermatids in stage V tubules (**Fig. 2**). The localization of drebrin E at the apical ES, however, shifted mostly to the concave side of the spermatid head in stage VII tubules and became considerably diminished at stage VIII. However, it remained restricted to the concave side of the apical ES at stages VII and VIII (**Fig. 2**). On the other hand, F-actin was found not only at the concave side of the apical ES; instead, it surrounded the entire spermatid head (**Fig. 2**) so that F-actin surrounded the entire apical ES, but drebrin E displayed a more restricted temporal and spatial expression at the apical ES, depending on the stage of the epithelial cycle. In short, drebrin E was more abundant at specific site at the apical ES namely the concave side of the apical ES, which is also the site where the cascade of endocytic vesicle-mediated protein trafficking events initiates, beginning at stage VII of the epithelial cycle. Interestingly, drebrin E, together with Eps8 and Arp3, were all temporally and spatially expressed, and restricted to the concave side of elongating spermatids in stages VII–VIII tubules, while F-actin was found to surround the entire elongating/elongated spermatid head at the apical ES. At stage VIII, the disruption of the F-actin network surrounding elongated spermatid heads to prepare for spermatid release coincided with a decrease in the expression of drebrin E, Eps8 and Arp3. These findings suggest that drebrin E may be working with other actin regulators such as Eps8 and Arp3 to regulate apical ES restructuring and to facilitate spermatid movement, orientation and spermiation.

Table 1. Source and working dilutions of antibodies used for various experiments in this report*

Target protein	Vendor	Catalog number	Lot number	Host species	Usage (Dilution)	Conjugation
Actin	Santa Cruz Biotechnology	sc-1616	H0808	Goat	IB (1:300)	/
SFKs		sc-8056	D0710	Mouse	IB (1:300)	/
Mouse IgG		sc-2371	/	Bovine	IB (1:3,750)	HRP
Rabbit IgG		sc-2370	/	Bovine	IB (1:3,750)	HRP
Goat IgG		sc-2350	/	Bovine	IB (1:3,750)	HRP
Drebrin**	Abcam	ab12350-50	445412, 706731	Mouse	IB (1:100)	/
		ab11068-50	653725, 956242	Rabbit	IB (1:1000); IF (1:100); IP (2 μg)	/
	Proteintech	10260-1-AP	/	Rabbit	IHC (1:100); IF (1:100)	/
Arp3	Sigma-Aldrich	A5979	114K4829	Mouse	IB (1:3,000); IF (1:200)	/
β-Catenin	Invitrogen	71-2700	564500A	Rabbit	IB (1:250)	/
Occludin		71-1500	636024A	Rabbit	IB (1:250)	/
Mouse IgG		A-11029	/	Goat	IF (1:250)	Alexa Fluor 488
Rabbit IgG		A-21429	/	Goat	IF (1:250)	Alexa Fluor 555
Eps8	BD Biosciences	610144	71332	Mouse	IB (1:5,000)	/
FAK	Millipore	06-543	DAM1770295	Rabbit	IB (1:1,000)	/

*Each antibody used for the studies reported herein cross-reacted with its corresponding protein in rat testis as indicated by the manufacturers. **The drebrin antibodies purchased from these two vendors cross-reacted with both drebrin A and E, but since testes, including Sertoli cells, were found to express only drebrin E (note: germ cells did not express any drebrins) by immunoblotting (see **Fig. 1A**), the drebrin antibodies thus detected only drebrin E in our experiments. Abbreviations: IB, immunoblot analysis; IF, immunofluorescence microscopy; IHC, immunohistochemistry; IP, immunoprecipitation; HRP, horseradish peroxidase.

Adjudin-induced apical ES restructuring causes a reduction of drebrin E that leads to a loss of spermatid polarity/orientation, as well as to premature spermatid release, mimicking "spermiation". Adjudin, a potential male contraceptive under investigation in our laboratory,[34-36] is known to induce premature loss of germ cells through a disruption of anchoring junctions between Sertoli and germ cells, most notably and initially at the apical ES, to be followed by the desmosome and the GJ at the Sertoli cell-pre-step 8 spermatid interface.[12,35,37] A mild but insignificant decline in the steady-state protein level of drebrin E was detected in the testis by 3-, 7- and 11 h post adjudin treatment, which is followed by a statistically significant decline by 1- and 2 d thereafter (**Fig. 3A**). Its protein level became virtually undetectable when germ cells were depleted from tubules at 4 d post-adjudin treatment.[38] But since drebrin E was shown to be expressed almost exclusively by Sertoli cells when examined by immunoblotting (see **Fig. 1A**), this reduction in drebrin E in the testis by 1–4 d after adjudin treatment reflected mostly the decline of drebrin expression by Sertoli cells since the Sertoli cell number was shown not to be affected by adjudin treatment.[34,39,40] These findings also suggest that drebrin E expression by Sertoli cells was dependent on the presence of germ cells.

The two upper parts in **Figure 3B** represent the expression and co-localization of drebrin E with F-actin in control rat testes, where drebrin was restricted to the concave side of the elongated spermatid heads in stage VI or VII tubules. However, by 7 h after adjudin treatment, mis-oriented elongating spermatids in stage VI–VII or VII tubules were noted (see white arrowheads in **Fig. 3B**), and these mis-oriented spermatids were in the process of being detached from the epithelium (**Fig. 3B**). Besides a concomitant decline in drebrin E and F-actin at elongating spermatids at these stages following adjudin treatment, drebrin E was also found to be mis-localized (**Fig. 3B**). Instead of being restricted to the concave side of the spermatid head, immunoreactive drebrin E was also found on the convex side of spermatid heads (see yellow arrowheads) in rats following treatment with adjudin (**Fig. 3B**). This is important since it suggests that proper localization of drebrin E at the apical ES may be necessary to confer spermatid orientation in the epithelium. Also, it was noted that the expression of drebrin E was considerably diminished at the apical ES in stage VII tubules by 7 h following treatment of adjudin vs. controls (**Fig. 3B**), consistent with the finding shown in **Figure 3A**. This was also reminiscent of the disruption of the F-actin network and the diminishing drebrin E expression around elongated spermatids at the apical ES during spermiation in stage VIII tubules. Hence, a decline of drebrin E expression at the apical ES is probably associated with its restructuring, preceding the sloughing of spermatids induced by adjudin or the natural sperm release as it occurs in normal rats at spermiation.

TNFα and TGFβ3 cause a transient decline in the drebrin E level in primary Sertoli cell cultures. When Sertoli cells were cultured in vitro at low cell density (0.005 x 10^6 cells/cm^2), drebrin E and F-actin were also found to co-localize at the cell edge (**Fig. 4A**), validating their co-localization at the cell-cell interface and at cell junctions shown in vivo. Sertoli cells were then cultured at a higher density (at 0.5 x 10^6 cells/cm^2) on Matrigel-coated dishes to form a functional TJ permeability barrier with ultrastructural characteristics corresponding to TJs, basal ES and desmosomes that resemble the BTB in vivo.[41,42] These cells were subjected to cytokine treatment which is known to induce junction restructuring via an increase in endocytic vesicle-mediated protein trafficking.[43-45] Both TNFα and TGFβ3, at concentrations that were known to induce disruption of the TJ permeability barrier,[46-48] were shown to induce a transient reduction

of drebrin E (**Fig. 4B and C**). This decrease in drebrin E subsequently returned to its basal level 24 h after treatment. However, the steady-state level of Arp3 in these same Sertoli cell cultures remained relatively stable, even though Arp3 was shown to bind drebrin E (see **Fig. 5**). These findings show that cytokine-induced disruption of the TJ permeability barrier may be mediated via its action on the actin binding protein drebrin E.

Identification of the binding partner(s) of drebrin E and changes in drebrin E-Arp3 interactions in the Sertoli cell epithelium following TNFα and TGFβ3 treatment. Co-immunoprecipitation (Co-IP) was used to identify the binding partner(s) of drebrin E using Sertoli cells cultured in vitro for 4 d at 0.5 x 10^6 cell/cm^2. Thus, at the time these cultures were harvested for lysate preparation for Co-IP, the cell epithelium mimicked Sertoli cells in vivo, that is, it contained ultrastructural features corresponding to TJs, basal ES, desmosomes and GJs, and a functional BTB. Interestingly, drebrin E was found to structurally interact with Arp3 (an actin nucleation/branching regulator), but not with Eps8 and other Sertoli cell proteins found at the BTB (**Fig. 5A**), illustrating drebrin E is involved in restructuring of actin filaments at the apical and basal ES by conferring actin branching. While cytokines (e.g., TNFα, TGFβ3) were found to transiently inhibit the production of drebrin E by Sertoli cells, a significant increase (by as much as ~2.5-fold) in the association between drebrin E and Arp3 was detected (**Fig. 5B and C**). These findings seemingly suggest that drebrin E, under the influence of cytokines at stage VIII of the seminiferous epithelial cycle, may be recruiting more Arp3 to induce actin nucleation/branching, thereby facilitating junction restructuring at the BTB and at the apical ES to facilitate the transit of preleptotene spermatocytes at the BTB and the release of spermatids near the luminal edge of the apical ES at spermiation.

Redistribution of drebrin E and changes in the F-actin network in the Sertoli cell epithelium following treatment of cells with TNFα and TGFβ3. To further understand the role of drebrin E in maintaining ES function via its effects on the actin network, Sertoli cells cultured at 0.0125 x 10^6 cells/cm^2 were treated with either TNFα (10 ng/ml) or TGFβ3 (3 ng/ml), which are known to perturb Sertoli cell TJ permeability barrier function,[46,48] and terminated at 4 h and 1 d thereafter to monitor their effects on the F-actin network. In control cells, drebrin E was found to localize to the Sertoli-Sertoli cell interface (see yellow arrowheads in **Fig. 6**) and to co-localize with F-actin. However, following treatment with either cytokine, F-actin became truncated and appeared to be defragmented in many Sertoli cells (see white arrowheads in **Fig. 6**) and the actin network at the cell periphery appeared to "pull" away from the cell-cell contact site (see red arrowheads in **Fig. 6**). These changes in F-actin were found to associate with a redistribution of drebrin E since virtually no drebrin E was found at the Sertoli-Sertoli cell interface following treatment with cytokine, suggesting that such changes in drebrin E redistribution affected the proper distribution of other actin regulatory proteins, such as Arp3. These results illustrate that a functional and/or properly organized F-actin network failed to be maintained within Sertoli cells after cytokine treatment.

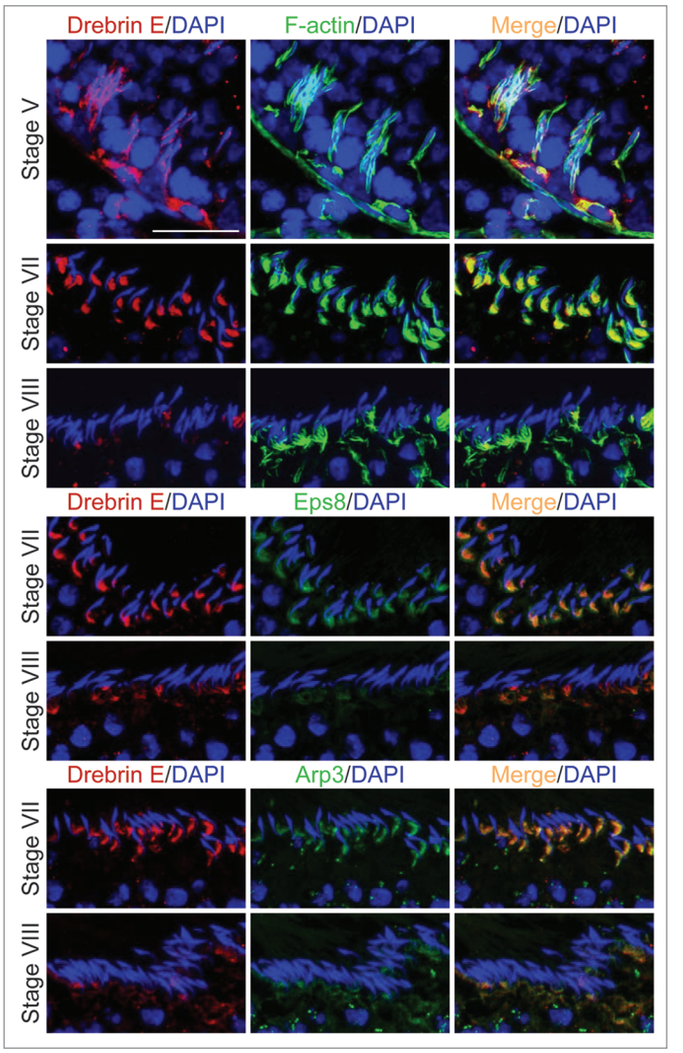

Figure 2. A study to examine the co-localization of drebrin E with F-actin and two other actin regulatory proteins, Eps8 and Arp3, in the seminiferous epithelium of adult rat testes. Drebrin E (red fluorescence) and F-actin (green fluorescence) were found to co-localize in the seminiferous epithelium of adult rat testes (orange-yellow fluorescence; see merged images on the right), consistent with their localization at the BTB, mostly at stage V, and also at the apical ES. Drebrin E was found at the apical ES, surrounding the entire heads of elongating spermatids at stage V, but its localization shifted and localized mostly on the concave side of elongating spermatids at the apical ES in stage VII tubules. Drebrin E also co-localized with two other actin regulators, namely Eps8 (green fluorescence) and Arp3 (green fluorescence), which are known to be present at the apical ES at stage VII. When the actin filament network at the apical ES undergoes restructuring at stage VIII of the seminiferous cycle, a considerable decline in the expression of drebrin, Eps8 and Arp3 was detected. Cell nuclei were visualized by DAPI staining. Bar = 50 μm, which also applies to the other micrographs. These findings are representative results from a single experiment, which was repeated three times using testes from different set of rats. Each experiment yielded similar results. Stages of the seminiferous epithelial cycle are denoted as Roman numerals to the left of images.

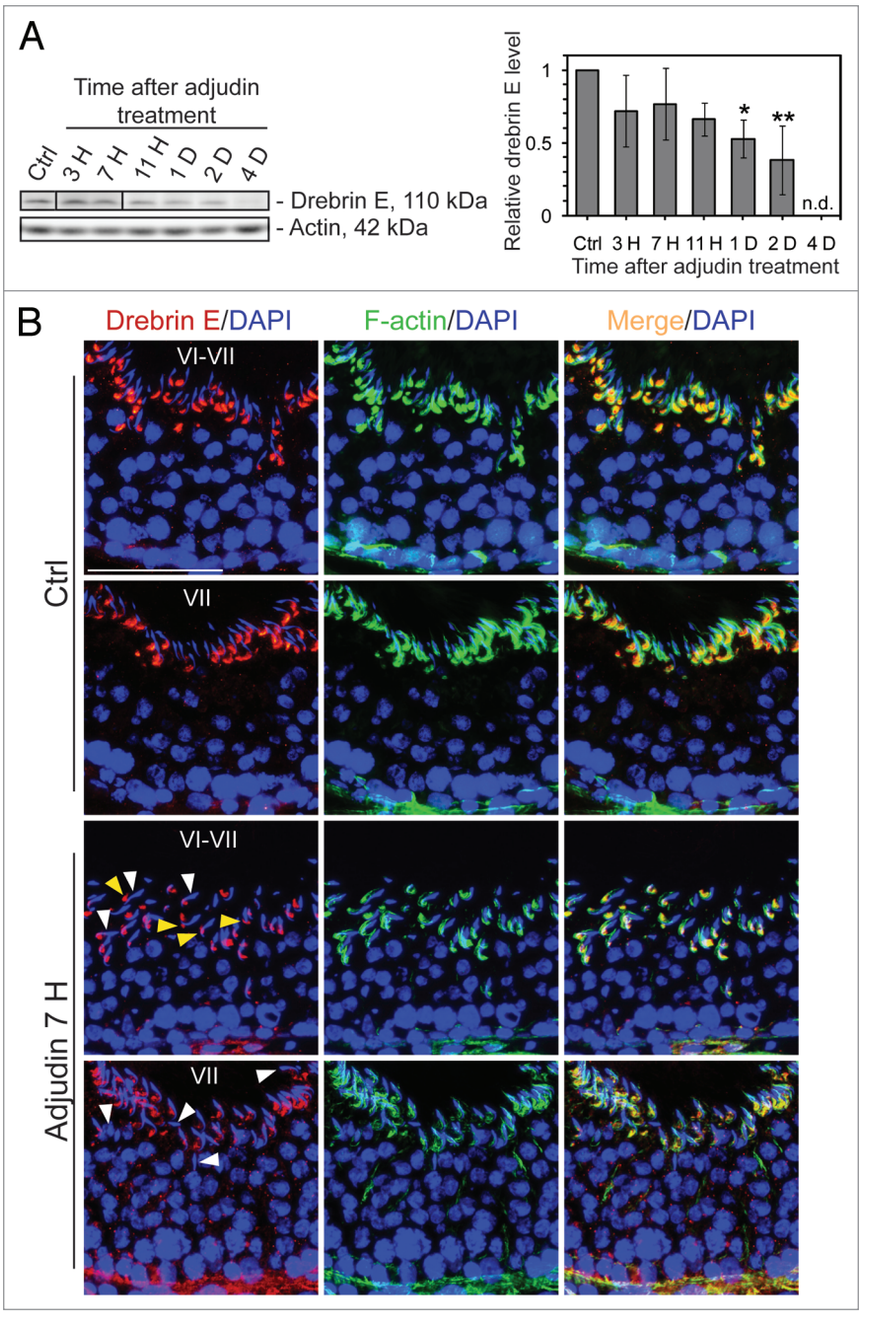

Figure 3. For figure legend, see page 129.

Changes in the distribution of drebrin E and Arp3 in the Sertoli cell epithelium following treatment of cells with TNFα and TGFβ3. To further expand the above findings which show that changes in F-actin dynamics are mediated by drebrin E via its interaction with Arp3, the following experiment was performed. Sertoli cells were treated with either TNFα or TGFβ3 for 4-h and changes in protein distribution in Arp3 and drebrin E were monitored by dual-labeled immunofluorescence analysis. It was noted that the distribution of Arp3 and drebrin E at the cell-cell interface (see yellow arrowheads) and in cell cytosol within Sertoli cells is important to maintain a functional F-actin network based on findings in control Sertoli cell epithelium (**Fig. 7 vs. 6**). However, following treatment of the Sertoli cell epithelium with either TNFα or TGFβ3 for 4-h, less drebrin E and Arp3 were found at the cell-cell interface, except that these proteins had internalized "together" (see **Fig. 7**), moving further into cell cytosol to surround the periphery of the nucleus (see the co-localization of Arp3 with drebrin E as visualized by "orange" fluorescence, red arrowheads) (**Fig. 7**). Since Arp3 is known to induce actin branching, this cytokine-induced change in Arp3 localization (see **Fig. 7**) (but not its expression/production, see **Fig. 4**) offers an explanation for the truncated and/or

Figure 3 (See opposite page). Apical ES disruption induced by adjudin is accompanied by a considerable reduction of drebrin E at the apical ES, but not at the BTB. (A) By immunoblotting, following adjudin treatment in adult rats (50 mg/kg b.w., one dose, by gavage) to induce premature loss of germ cells, a decline in the steady-state level of drebrin E was detected in the testis, beginning from 1 d (day) post-treatment and almost non-detectable by 4 d when virtually all elongating/elongated spermatids were depleted from the epithelium. Actin served as loading control against which the drebrin E was normalized. Histogram is shown on the right part which summarized immunoblotting data shown on the left part with each bar = mean ± SD from n = 3 rats. The steady-state level of drebrin E in control rats was arbitrarily set at 1. *$p < 0.05$; **$p < 0.01$. n.d., not detectable. (B) In the control testis, drebrin E (red fluorescence) was detected at the concave side of elongating/elongated spermatid heads in stage VI and VII tubules, but F-actin (green fluorescence) was found surrounding the entire apical ES. Cell nuclei (blue) were visualized by DAPI staining. At about 7 h (hour) post-adjudin treatment when premature loss of elongating/elongated spermatids began to occur, a lowered and also truncated protein expression of drebrin E and F-actin were detected at the apical ES in non-stage VIII tubules when examined by immunofluorescence microscopy in which the staining of drebrin E and actin appeared to be "broken" and "defragmented." Furthermore, many elongating spermatids in adjudin-treated rats were found to be mis-oriented with their heads no longer pointing toward the basement membrane (see "white" arrowheads). In these mis-oriented elongating spermatids, drebrin E was also found to be mis-localized, which was no longer restricted to the concave side of the spermatid head; instead, it was found on the convex side of the spermatid head (see "yellow" arrowheads), perhaps binding to the Arp2/3 complex to induce protein nucleation and to cause disruption of actin filament bundles, thereby causing actin branching. The net result of these changes induces "premature" apical ES disruption, thereby leading to germ cell depletion from the seminiferous epithelium. While the level of expression of drebrin E and F-actin at the basal ES at the BTB in stage VI and VII tubules by 7 h after adjudin treatment remained relatively similar to control (normal) rats, the drebrin E level was found to be enhanced considerably in stage VII in adjudin treated rats vs. control. Bar = 100 μm, which also applies to all other micrographs.

defragmented F-actin configuration found in Sertoli cell cytosol as illustrated in **Figure 6**, and also for the formation of the branched F-actin network at the cell periphery (see red arrowheads in **Figure 6** vs. 7).

Discussion

Drebrin E in regulating junction dynamics during spermatogenesis. Drebrin has been implicated in the regulation of cell adhesion since it was demonstrated to stabilize connexin 43 (Cx43)-containing GJ plaques, possibly serving as an adaptor of the actin cytoskeleton[49] by recruiting or modulating the activity of other actin regulatory proteins, such as Esp8 and the Arp2/3 complex, which confer actin filament bundling and branching, respectively.[15,50-53] Cx43 was shown recently to be involved in junction restructuring at the BTB, particularly in the reassembly of the TJ-barrier following its disruption,[38,54] which occurs during the transit of preleptotene spermatocytes at stage VIII of the epithelial cycle. Thus, it was tempting to speculate that drebrin E is participating in these events by recruiting actin regulatory proteins, such as Arp3 to the apical and/or the basal ES since Arp3 was shown to be a binding partner of drebrin E as demonstrated herein. Furthermore, based on the stage-specific expression pattern of drebrin E and its restricted temporal and spatial expression in the seminiferous epithelium during the seminiferous epithelial cycle, drebrin E may be involved in the restructuring of the apical and basal ES via its protein recruitment capability. For instance, drebrin E expression was highest at the concave side of the elongating spermatid head at stages VI-VII, which is the site formerly known as the tubulobulbar complex to be formed at stage VIII of the epithelial cycle.[55] Recent studies have shown this site to be the apical ES where endocytic vesicle-mediated protein trafficking events begins at late stage VII of the epithelial cycle[56] so that "old" apical ES proteins (e.g., N-cadherin, nectins, JAM-A) can be endocytosed, transcytosed and recycled for assembly of the "new" apical ES that arises during spermiogenesis at the interface of Sertoli cell and step 8 spermatid.[1,33,53] These events are also necessary to confer spermatid polarity so that the heads of developing spermatids can point toward the basement membrane during spermiogenesis, which essentially packs a maximal number of developing spermatids in the seminiferous epithelium. This hypothesis is supported by recent findings which showed clathrin, N-WASP and cortactin to be highly expressed at the concave side of the spermatid head at stage VII and to be involved in endocytic vesicle-mediated trafficking of proteins.[57] This hypothesis is also supported by findings herein which illustrated a mislocalization of drebrin E and a decrease in its steady-state level 7-h after adjudin treatment. In short, drebrin E is probably working in concert with other proteins at the "degenerating" apical ES to prepare for sperm release at spermiation, and once the necessary actin network is "prepared" for spermiation, the expression of drebrin E decreases considerably, similar to the actin bundling protein Eps8.[19] This speculation is also consistent with findings using the adjudin model since a significant decline in drebrin E at the "degenerating" apical ES was detected, thereby allowing immature spermatids to undergo "unwanted spermiation" in non-stage VIII tubules because of F-actin disorganization at the apical ES. This concept is also applicable to BTB restructuring since a transient disappearance in drebrin E was noted at the BTB at stages VII-VIII, similar to its disappearance at the apical ES at stage VIII to facilitate sperm release. This concept is further supported by the observation that treatment of the Sertoli cell epithelium with either TNFα or TGFβ3 led to a redistribution of drebrin E. This in turn affected the proper distribution of F-actin filaments in Sertoli cells. Since cytokines (e.g., TNFα, TGFβ3) produced by Sertoli and/or germ cells within the BTB microenvironment[1,33,58] at stage VIII, while capable of reducing the drebrin E steady-state level (see **Fig. 4**), can enhance the interaction between drebrin E and Arp3 (see **Fig. 5**), thereby increasing the presence of the Arp2/3 complex at the BTB. This would cause truncation and disruption of actin filament bundles via its effects on actin branching (see **Figs. 6 and 7**), providing a favorable environment for endocytic vesicle-mediated endocytosis. The net result of these cellular events would destabilize junctions at the BTB and facilitate the transit of preleptotene spermatocytes.

Crosstalk of drebrin with other actin regulators at the apical ES. In neuronal cells, various studies have demonstrated the role of drebrin in F-actin reorganization.[26,32] Drebrin is associated

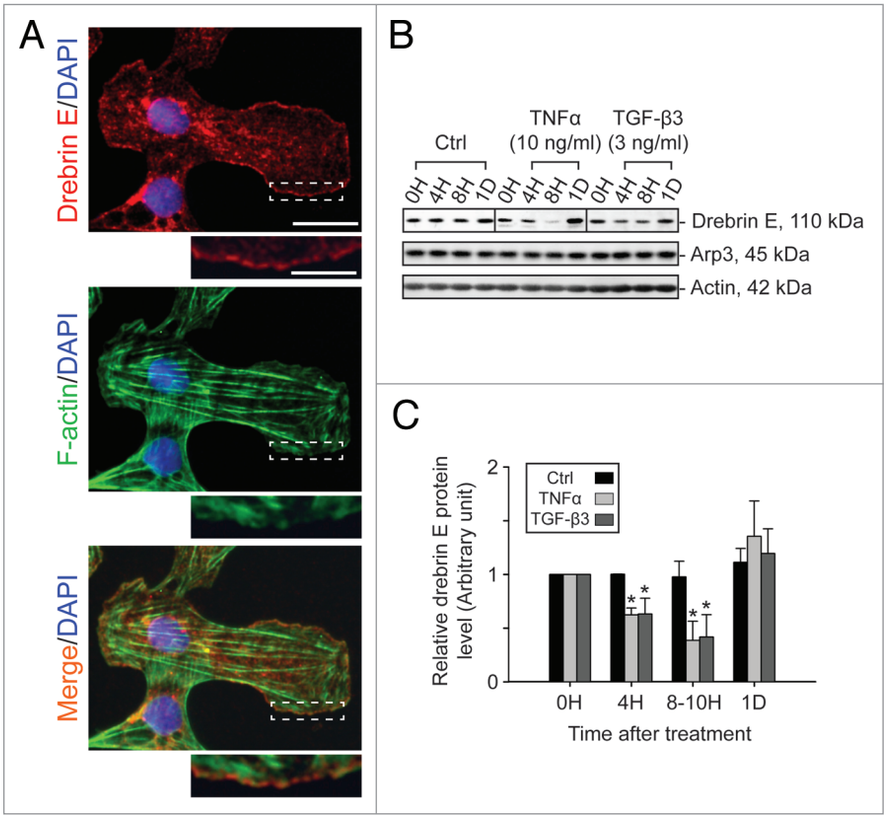

Figure 4. Localization of drebrin E in Sertoli cells cultured in vitro and cytokine-induced transient decline of the drebrin E steady-state protein level in the Sertoli cell epithelium. (A) When Sertoli cells were cultured at 0.005 x 10^6 cells/cm^2 for 4 d on Matrigel-coated coverslips and stained for drebrin E (red fluorescence), drebrin E localized to the cytoplasm, as well as to the plasma membrane near the cell surface. Drebrin E, an actin regulator, also co-localized with F-actin (green fluorescence) but mostly at or near the cell surface (see inset below each micrograph, which is a magnified view of the area enclosed within the "broken-line" rectangle). Bar = 40 μm in the top micrograph, which also applies to the other micrographs; bar in inset = 15 μm in the top micrograph, which also applies to the other insets. (B and C) Sertoli cells were cultured at 0.5 x 10^6 cells/cm^2 on Matrigel-coated dishes for 4 d, forming an intact epithelium with an established TJ permeability barrier and ultrastructural features corresponding to TJs, basal ES, GJs and desmosomes, mimicking the Sertoli cell BTB in vivo.[41,42] On day 4, Sertoli cells were treated with either TNFα (10 ng/ml) or TGFβ3 (3 ng/ml) vs. controls (no treatment) and cultures were terminated at 4 h (hr), 8–10 h and 1 d (day) thereafter. Previous studies have shown that these cytokines induced junction restructuring at the BTB, disrupting the Sertoli cell TJ-permeability barrier.[46,47,78] A transient but statistically significant decline in the steady-state protein level of drebrin E was detected at 4 h to 8–10 h after TNFα or TGFβ3 treatment vs. the control. However, this decline in drebrin E level returned to its basal level by 24 h post-treatment. While Arp3 was shown to be a binding partner of drebrin E (see **Fig. 5**), the steady-state of Arp3 remained altered throughout the entire experimental period following treatment with cytokine vs. the control (B). Actin served as the protein loading control against which scanned data of drebrin E were normalized. The immunoblotting data shown in (B) illustrate changes in the protein level of drebrin E following cytokine treatment after images were densitometrically scanned using Multi Gauge software and shown in the histogram depicted in (C). Scanned data of Arp3 normalized against actin following cytokine treatment vs control were not shown in (C) because no significant changes were detected. Each bar = mean ± SD from six different culture experiments using different batches of Sertoli cells. 8–10 h indicates cultures were terminated at either 8 (n = 3) or 10 (n = 3) H after treatment with cytokine. The steady-state level of drebrin E at 0 h was arbitrarily set at 1. *$p < 0.05$.

with changes in cell shape and actin plasticity. It was reported that the magnitude of changes in cell shape correlated with the level of drebrin overexpression.[26] This thus suggests interaction of drebrin with other proteins during F-actin reorganization. The high level of drebrin E expression at the concave side of elongating spermatids at stage VII may thus be necessary for F-actin remodeling, such as by recruiting other actin regulatory proteins to the site to facilitate sperm release at stage VIII of the epithelial cycle. Similarly, the elevated expression of drebrin E at the BTB at stages V and VI may also be needed to prepare for the transit of preleptotene spermatocytes across the barrier at stages VII and VIII of the epithelial cycle. Drebrin E, with its F-actin binding property and ADF-H domain, was suggested to regulate the F-actin network by its competitive binding with other actin depolymerizing proteins and/or factors, such as α-actinin, fascin and tropomyosin.[32] Lowered drebrin level and a disrupted actin network were observed in brains during Alzheimer disease.[59,60] The loss of drebrin in dendritic spines due to reduced PAK (p21-activated kinase, which is also a component of the β1-integrin-based protein complex at the apical ES[41,60a]) was shown to lead to an increase in cofilin (an actin severing protein) binding to F-actin, and thus a disrupted F-actin network.[60] Thus, the considerably reduced drebrin E expression at the apical ES at the concave side of the spermatid heads at stage VIII of the epithelial cycle may promote the binding of F-actin depolymerizing factor(s) (e.g., cofilin) to F-actin and facilitate the necessary actin

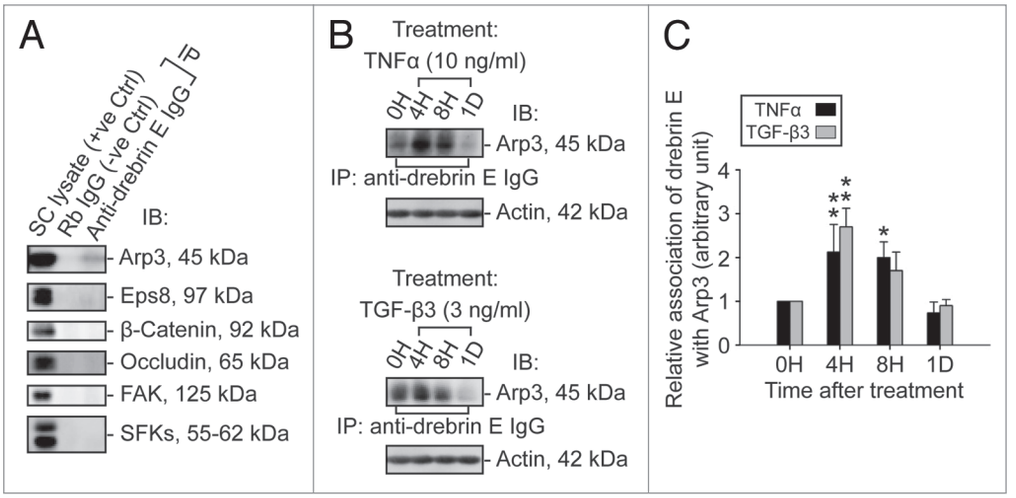

Figure 5. A study by co-immunoprecipitation (Co-IP) to identify the binding partner(s) of drebrin E and changes in the interaction between drebrin E and Arp3 in the Sertoli cell epithelium following treatment with cytokines. (A) Sertoli cells were cultured at 0.5 x 10^6 cells/cm^2 for 4 d to allow the formation of a functional TJ-permeability barrier with ultrastructural features corresponding to TJs, basal ES, GJs and desmosomes when examined by electron microscopy.[41,42,76] Thereafter, lysates were obtained by using IP lysis buffer and about 250 μg protein from each sample was used for Co-IP. The column on the left is positive control using Sertoli cell lysates (25 μg protein) per lane alone without Co-IP. Negative control (-ve Ctrl) was prepared using normal rabbit IgG instead of the anti-drebrin E IgG for Co-IP. It was found that drebrin E associated with Apr3, but not Eps8, β-catenin, occludin, FAK or Src family kinases as demonstrated in this representative experiment which was repeated three times using lysates from different batches of Sertoli cell cultures. (B and C) This Co-IP experiment was performed using samples similar to those shown in Figure 4B. In brief, Sertoli cells cultured for 4 d were treated with either TNFα or TGFβ3 for 4 h (hr), 8 h and 1 d (day). About 250 μg total protein from each sample was used for Co-IP with an anti-drebrin E antibody and the resulting immunocomplexes were examined by immunoblotting using anti-Arp3 antibody. Actin served as the protein loading control. It was noted that while there was a significant loss of drebrin E steady-state level at 4 and 8 h by about 50% (see **Fig. 4B and C**), there was a ~2- to 3-fold increase in the association between drebrin E and Arp3 following treatment with either TNFα or TGFβ3 (B). In (C), each bar = mean ± SD of n = 3 from three independent experiments. The amount of drebrin E associated with Arp3 at time 0 was arbitrarily set at 1. *p < 0.05; **p<0.01.

reorganization for sperm release at spermiation. This possibility was also supported by the findings reported herein regarding the similar stage-specific, cellular localization and co-localization, and highly restricted temporal and spatial expression of drebrin E vs. Eps8 [19] and Arp3 [20] in the seminiferous epithelium. It is possible that drebrin E recruits actin regulators to the apical ES to initiate the cascade of events leading to the disorganization of actin filament bundles at the basal and apical ES which begins at stage VII, thereby allowing sperm release to occur at stage VIII of the epithelial cycle. This possibility is indeed supported by our findings which show Arp3 to bind drebrin E at the Sertoli cell BTB.

Cytokine treatment affects drebrin E expression and Arp3 distribution in the Sertoli cell epithelium. Cytokines, such as TGFβ3, TNFα and IL-1α, are known to regulate cell adhesion at the BTB[48,61-63] by facilitating endocytic vesicle-mediated protein trafficking events.[43,44,64] Even though drebrin E per se was not highly expressed at the BTB during restructuring of the immunological barrier at stage VIII of the epithelial cycle (but only at stages V and VI of the cycle as shown herein) when transit of preleptotene spermatocytes at the BTB occurs,[14,65,66] the steady-state level of drebrin E was shown to be regulated by cytokines. Also, cytokines are known to be produced stage-specifically by Sertoli and/or germ cells in the seminiferous epithelium during the epithelial cycle.[67-69] Thus, the localized production of cytokines within the microenvironment of the BTB can regulate the level of drebrin E to fine tune the homeostasis of actin filament bundles at the basal ES and perhaps the apical ES as well, to regulate the integrity of the ES during the epithelial cycle. It is likely that this event is tightly associated with the restricted temporal and spatial expression of Eps8 and Arp3 (and possibly other actin regulatory proteins). Indeed, following treatment of the Sertoli cell epithelium with cytokine, there was a significant increase in the association of drebrin E and Arp3, and Arp3 is known to induce F-actin nucleation,[15] causing the formation of a branched actin network from actin filament bundles, thereby destabilizing the BTB. Thus, while there is an overall decline in drebrin E at the BTB, significantly more Arp3 can be "recruited" to this site to elicit actin network branching, conferring cell plasticity to facilitate the transit of preleptotene spermatocytes across the barrier. This possibility, however, will need to be confirmed in future functional studies, such as by using RNAi to knockdown drebrin E to examine its impact on Sertoli cell barrier function and to assess changes in the distribution of Arp3, Eps8 and other BTB proteins. Nonetheless, we have demonstrated that treatment of Sertoli cells having a functional tight junction barrier that mimics the BTB in vivo by cytokine, either TNFα or TGFβ3, can affect the distribution of Arp3 and drebrin E (even though the steady-state level of Arp3 in these cultures was not altered), moving these proteins from the Sertoli-Sertoli cell interface and into the cell cytosol. Thus, this affects the F-actin configuration, causing truncation of the actin network in the cell cytosol and also the formation of a branched actin network at the cell periphery. In short, following treatment of the Sertoli cell epithelium

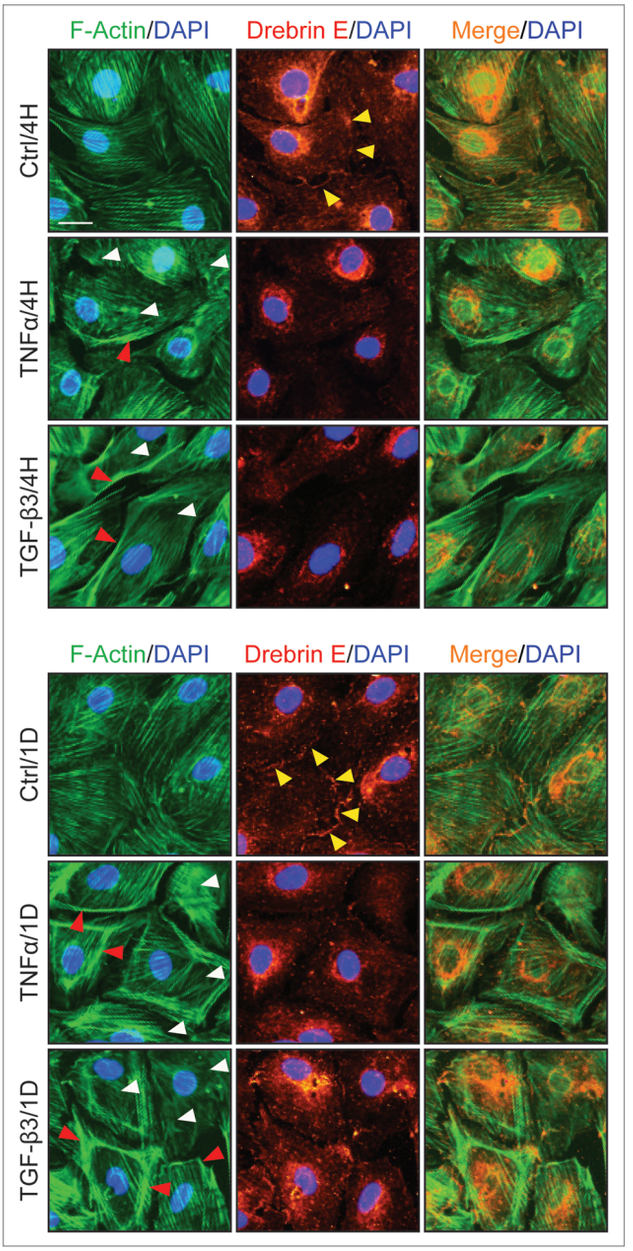

Figure 6. A study by dual-labeled immunofluorescence analysis to assess the effects of cytokines on the actin filament cytoskeleton and the distribution of drebrin E in Sertoli cells. Sertoli cells were cultured at 0.0125 x 10^6 cells/cm^2 on Matrigel-coated coverslips in F12/DMEM for 4 d at 35°C with 5% CO_2/95% air (v/v) in a humidified atmosphere prior to treatment. This cell density was selected to ensure that Sertoli cell nuclei would be evenly distributed and changes in drebrin E (red fluorescence) and F-actin (green fluorescence) filament distribution at the Sertoli-Sertoli cell interface and cell cytosol would be readily visible. Also, at this cell density, ultrastructures of TJ, basal ES, desmosome, and GJ were detected at the Sertoli-Sertoli cell interface under electron microscopy, illustrating functional junctions were established in these cell epithelia as detailed elsewhere.[38,54,77] It was noted that in the control Sertoli cells, F-actin formed an extensive network of filaments, which was used to maintain proper cell shape. Drebrin E was detected at the Sertoli-Sertoli cell interface (see "yellow" arrowheads in middle column) and in the cell cytosol. Co-localization of drebrin E was detected in the cell cytosol, surrounding the cell nucleus, as well as at the cell-cell interface. These findings are also consistent with findings shown in Figure 4A. However, following treatment of Sertoli cells with either TNFα or TGFβ3 for 4 h (hr), actin filaments were found to become truncated and appeared defragmented with some actin filaments being disrupted (see "white" arrowheads). Additionally, actin filaments at the cell-cell interface appeared to move away from the cell-cell interface, forming actin bundles at the cell periphery (see "red" arrowheads) after treatment of the Sertoli cell epithelium with cytokines for 1D (day). Also, drebrin E no longer co-localized with F-actin at the cell-cell interface (see merged images in both treatment groups vs. control group) and drebrin E was localized mostly in Sertoli cell cytosol. Sertoli cell nuclei were visualized by DAPI staining (blue). These micrographs are representative findings from one experiment, but this experiment was repeated three times using different batches of Sertoli cells, which yielded similar results. Bar = 30 μm, which applies to all micrographs.

with cytokine, drebrin E recruits Arp3 to the appropriate cellular sites to destabilize the scaffolding function of actin, which also facilitates endocytic vesicle-mediated protein endocytosis to destabilize the TJ permeability barrier. This is likely what is occurring at stage VIII of the epithelial cycle when barrier function needs to be destabilized to facilitate the transit of preleptotene spermatocytes.

Materials and Methods

Animals. Sprague-Dawley rats were purchased from Charles River Laboratories (Kingston, NY) and housed at the Comparative Bioscience Center of the Rockefeller University. All rats were housed with a light:dark cycle of 12 hr:12 hr with free access to standard chow and water at 22 ± 1°C. The use of animals for all of the experiments reported herein was approved by the Rockefeller University Institutional Animal Care and Use Committee with Protocol Number 09016.

Chemicals and antibodies. All chemicals and reagents were purchased from Sigma-Aldrich (St. Louis, MO) unless otherwise specified. Antibodies used for different experiments (such as immunoblotting and dual-labeled immunofluorescence analysis) were obtained from different vendors, and their working dilutions are listed in **Table 1**.

Adjudin treatment to induce anchoring junction restructuring in the testis. Adult Sprague-Dawley rats (~250–300 g body weight) received a single oral dose of adjudin (50 mg/kg body weight) as detailed elsewhere.[34,39] This treatment is known to induce restructuring of junctions in the seminiferous epithelium, mostly notably the apical ES which is then followed by the desmosome and gap junction.[3,34,36,37] When virtually all germ cells (except spermatogonial stem cells and spermatogonia) are depleted from the seminiferous epithelium, restructuring also occurs at the basal ES at the BTB.[40] Untreated rats served as the control.

Primary Sertoli cell cultures and cytokine treatment. Sertoli cells were isolated from testes of 20-d-old Sprague-Dawley rats as earlier described.[72] By 20 d of age, these Sertoli cells were differentiated and had ceased to divide. Moreover, they displayed morphological and functional properties indistinguishable from Sertoli cells isolated from adult rat testes using the BSA gradient method as detailed elsewhere.[47,73] Freshly isolated Sertoli cells were plated on Matrigel (BD Biosciences)-coated multiwell plates at 0.5 x 10^6 cells/cm^2 or on round

coverglasses at 0.005 x 10^6 cells/cm^2 or 0.0125 x 10^6 cells/cm^2. Cells were cultured in serum-free DMEM/F12 containing 10 μg/ml bovine insulin, 5 μg/ml transferrin (Calbiochem/EMD Chemicals), 2.5 ng/ml epidermal growth factor and 5 μg/ml bacitracin at 35°C in a humidified atmosphere of 5% CO_2/95% air (v/v) as earlier described.[74] Cells were hypotonically treated with 20 mM Tris (Invitrogen) (pH 7.4 at 22°C) on day 2 to lyse residual germ cells.[75] Sertoli cell purity in these cultures was >98% with negligible contamination of germ (e.g., spermatogonia and spermatocytes), peritubular myoid and Leydig cells, as earlier characterized by RT-PCR and immunoblotting using specific primer pairs or antibodies against corresponding marker genes/proteins and electron microscopy.[41,42,76] It should be noted that by ~day 2–3 these cells formed an intact epithelium and established a functional Sertoli cell TJ-permeability barrier when quantified by transepithelial electrical resistance (TER) across the cell epithelium. Ultrastructural characteristics typical of TJs, basal ES, desmosomes and GJs were also noted when Sertoli cells were examined by electron microscopy, mimicking the Sertoli cell BTB in vivo. On day 5, Sertoli cells were treated with 10 ng/ml recombinant rat TNFα or 3 ng/ml recombinant human TGFβ3 (R&D Systems) to assess the drebrin E level. These concentrations of cytokines were selected based on earlier studies from this laboratory.[44,46-48]

Immunoblot analysis. Protein lysates were prepared in Nonidet-P40 (NP40) lysis buffer [50 mM Tris (Invitrogen), 0.15 M NaCl, 10% glycerol (v/v), 1% NP40 alternative (v/v, Calbiochem), 2 mM EGTA, pH 8 at 22°C] freshly supplemented with protease and phosphatase inhibitor cocktails as earlier described.[76] Each sample was sonicated on ice for 10 sec twice using a Cole Palmer Model 4710 sonicator and then kept on ice for an additional 10 min with occasional vortexing to facilitate solubilization. After centrifugation at 15,000 g for 15 min, supernatants were collected. Protein concentration was estimated using the D_C protein assay kit (Bio-Rad Laboratories) and a BioRad Model 680 spectrophotometer. Antibodies used for detection of proteins by immunoblotting are listed in **Table 1**. Cytoskeletal proteins, namely actin and/or vimentin, served as protein loading controls. Chemiluminescent images were captured with a Fujifilm LAS-4000 mini luminescent image analyzer. Densitometry of non-saturated immunoblot images was analyzed with Multi Gauge software (Version 3.0, Fujifilm). In selected experiments, scanned image data obtained by Multi Gauge were reassessed and verified by Scion Image (Version 4.03, Scion Corp.).

Co-immunoprecipitation. Co-immunoprecipitation (Co-IP) was used to identify the binding partner(s) of drebrin E. Co-IP was performed essentially as earlier described,[77] using Sertoli cell lysates where cells (0.5 x 10^6 cells/cm^2) were cultured alone for 4 d with a hypotonic treatment performed ~36-h after cell plating to lyse residual germ cells. By day 4, these cultures were found to have a functional TJ permeability barrier when assessed by TER measurements across the cell epithelium.[54] Ultrastructural features corresponding to TJs, basal ES, GJs and desmosomes were also visualized by electron microscopy as described.[41] Sertoli cell lysates were obtained by using IP lysis buffer [10 mM Tris, 0.15 M NaCl, 1% NP-40 (v/v) and 10% glycerol (v/v), pH 7.4 at 22°C supplemented with protease and phosphatase inhibitor cocktails (Sigma-Aldrich) which were added at 1:100 immediately before its use]. About 250 μg protein was used from each sample for Co-IP which was performed as detailed elsewhere.[38,77] All samples within a given Co-IP experiment were processed simultaneously in an experimental session to avoid inter-experimental variations.

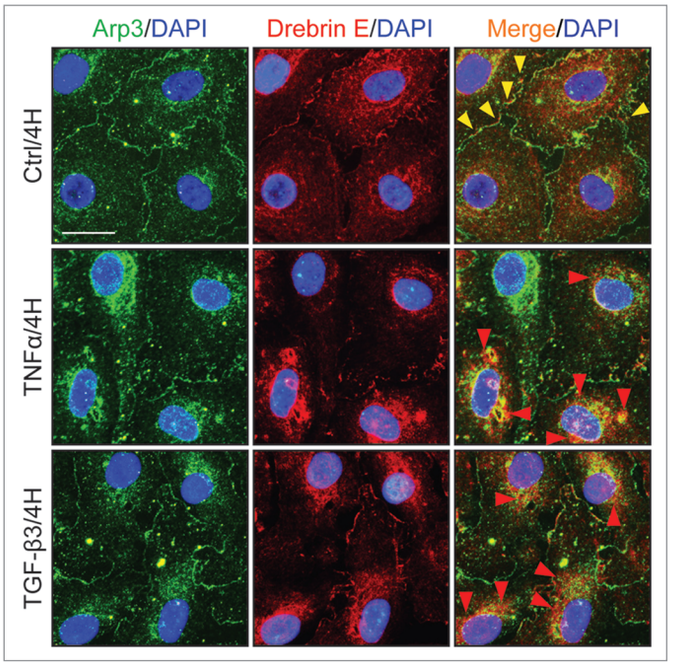

Figure 7. A study by dual-labeled immunofluorescence analysis to assess the effects of cytokines on the distribution of Arp3 and drebrin E in Sertoli cells. Sertoli cells cultured alone at 0.0125 x 10^6 cells/cm^2 on Matrigel-coated coverslips in F12/DMEM for 4 d, forming an epithelium. Thereafter, cells were treated with either TNFα or TGFβ3 for 4 h (hr) including control (Ctrl, no treatment) and terminated for dual-labeled immunofluorescence analysis. Consistent with findings shown in **Figures 4 and 6**, drebrin E (red fluorescence) was found at the Sertoli-Sertoli cell interface and in the cell cytosol, similar to Arp3 (green fluorescence) and some co-localization (see orange-yellow fluorescence in merged images) was found between Arp3 and drebrin E (see yellow arrowheads at the cell-cell interface), consistent with Co-IP data (**Fig. 4**). After cytokine treatment, drebrin E was found to undergo re-distribution, moving closer to cell nuclei and Arp3 also displayed a similar pattern of protein redistribution. Additionally, an increase in the co-localization of drebrin E and Arp3 was detected (see red arrowheads), consistent with findings of **Figure 4** which showed that an increase in protein-protein interactions between Arp3 and drebrin E was detected by 4 H following either TNFα or TGFβ3 treatment using the technique of Co-IP. Sertoli cell nuclei were visualized by DAPI staining (blue). Bar = 20 μm, which also applies to all other micrographs.

Immunohistochemistry. Immunohistochemistry was performed essentially as earlier described,[77] with minor modifications using frozen cross-sections of testes obtained with a cryostat at -20°C (~7-μm), collected on poly-L-lysine coated microscope slides (Polysciences, Warrington, PA) and fixed in Bouin's fixative (Polysciences). All treatment vs. control groups from a single experimental set were processed simultaneously and all cross-sections were collected on a minimal number of slides to avoid

inter-experimental variations. Endogenous peroxidase activity was quenched with 3% hydrogen peroxide (v/v) in methanol and cross-sections were permeabilized with 0.1% Triton-X100 (v/v) in PBS (10 mM sodium phosphate, 0.15 M NaCl, pH 7.4 at 22°C). After an overnight incubation with the anti-drebrin E antibody (see **Table 1**) or normal rabbit IgG (negative control) at room temperature, sections were incubated with a HRP (horseradish peroxidase) polymer conjugate that was specific for rabbit (and also mouse, guinea pig and rat) primary polyclonal antibody as instructed by the manufacturer's protocol in the SuperPicTure™ polymer detection kit (Invitrogen). Drebrin E immunoreactivity was visualized with 3-amino-9-ethylcarbazole (AEC, produced a reddish-brown precipitate). Thereafter, sections were post-stained with hematoxylin and slides were mounted with Clearmount™ mounting solution (Zymed Lab/Invitrogen). Micrographs were acquired with an Olympus DP71 digital camera (with a resolution of 12.5 Mpx) attached to an Olympus BX61 fluorescent microscope.

Immunofluorescence microscopy and dual-labeled immunofluorescence analysis. Fluorescence microscopy was performed utilizing cross-sections of frozen testes (obtained with a cryostat at -20°C) or cultured Sertoli cells. Testis cross-sections (7 μm) and cultured Sertoli cells (day 4 to 5 in vitro) were fixed with 4% paraformaldehyde (w/v) in PBS and permeabilized with 0.1% Triton X-100 (v/v) in PBS. Primary antibodies (see **Table 1**) were diluted at 1:100 in 1% bovine serum albumin (w/v, BSA) or normal goat serum (v/v, NGS) in PBS. Samples were incubated in primary antibody at room temperature overnight (see **Table 1**). After washing, samples were incubated for 30 min with secondary antibodies (see **Table 1**), which were diluted at 1:300 in 1% BSA or 10% NGS. For F-actin staining, samples were incubated for 30 min with phalloidin-FITC (6.6 μM), which was diluted at 1:200 in 1% BSA. After an additional washing step, samples were mounted with ProLong Gold Antifade solution with DAPI (4',6-diamidino-2-phenylindole, to visualize cell nuclei) (Invitrogen) and stored at 4°C. Fluorescent images were acquired by using an Olympus BX61 fluorescent microscope equipped with an Olympus DP71 digital camera and an HP xw8400 Workstation running MicroSuite Five imaging software (Olympus). Fluorescent images were overlaid using Adobe PhotoShop CS3 software for co-localization analysis.

General methods and statistical analyses. Electron microscopy was performed at the Rockefeller University Bio-Imaging Resource Center to confirm the presence of ultrastructures of TJ, GJ and desmosome in Sertoli cell cultures as detailed elsewhere.[76] The establishment of a functional TJ-permeability barrier in the Sertoli cell epithelium was assessed by TER across the cell epithelium by culturing Sertoli cells on bicameral units as described.[38,54,76] GB-STAT statistical analysis software (Version 7.0, Dynamic Microsystems) was used for statistical analyses. Each experiment was repeated at least 3 times. Statistical significance was analyzed with one-way analysis of variance (ANOVA), which was followed by the Tukey/Kramer post-hoc test. Values represent mean ± SD of n = 3–5 using different rats or different batches of Sertoli cell cultures. All experiments were performed 3–5 times to obtain enough replicates for meaningful statistical analysis, excluding pilot experiments which assessed and optimized different experimental conditions.

Concluding Remarks and Summary

In this study, the role of drebrin E in junction dynamics during spermatogenesis was examined. Drebrin E was found to display a restricted temporal and spatial expression pattern in the seminiferous epithelium, closely mimicking the localization of Arp3[20] and Eps8,[19] such as its enhanced expression at the concave side of elongating spermatids at the apical ES at stages VI–VII of the epithelial cycle, possibly for the recruitment of other actin regulators (e.g., Arp3) to prepare for F-actin restructuring at stage VIII. The significant decline in drebrin E at the ES at stage VIII also allows the binding of actin depolymerizing factors (e.g., tropomyosin, cofilin) to F-actin to induce "debundling" of actin filaments at both the apical ES and basal ES to facilitate spermiation and BTB restructuring, respectively. We have also shown that Arp3 is a binding partner of drebrin E and that cytokine-induced BTB disruption may be mediated via its effects on drebrin E expression and distribution at the Sertoli cell BTB in the seminiferous epithelium. Future studies should include the identification of other binding partners of drebrin E, such as palladin which is a known actin bundling protein.[70,71]

Acknowledgments

This work was supported in part by grants from the National Institutes of Health (NICHD, R01 HD056034 and R01 HD056034-02-S1 to C.Y.C.; U54 HD02990 Project 5 to C.Y.C.; R03 HD061401 to D.D.M.), and Hong Kong Research Grants Council (RGC) and CRCG Small Project Fund, University of Hong Kong (to W.M.L.; RGC grant HKU772009 and HKU773710 to W.Y.L.).

References

1. Cheng CY, Mruk DD. A local autocrine axis in the testes that regulates spermatogenesis. Nat Rev Endocrinol 2010; 6:380-95; DOI: 10.1038/nrendo.2010.71.
2. Cheng CY, Mruk DD. Cell junction dynamics in the testis: Sertoli-germ cell interactions and male contraceptive development. Physiol Rev 2002; 82:825-74. DOI: 10.1152/physrev.00009.2002
3. Mruk DD, Cheng CY. Sertoli-Sertoli and Sertoli-germ cell interactions and their significance in germ cell movement in the seminiferous epithelium during spermatogenesis. Endocr Rev 2004; 25:747-806; DOI: 10.1210/er.2003-0022.
4. O'Donnell L, Robertson KM, Jones ME, Simpson ER. Estrogen and spermatogenesis. Endocr Rev 2001; 22:289-318; DOI: 10.1210/er.22.3.289.
5. O'Donnell L, Meachem SJ, Stanton PG, McLachlan RI. Endocrine regulation of spermatogenesis. In: Neill JD Ed. Physiology of Reproduction. Amsterdam, Elsevier 2006; 3:1017-69.
6. Carreau S, Hess RA. Oestrogens and spermatogenesis. Philos Trans R Soc Lond B Biol Sci 2010; 365:1517-35; DOI: 10.1098/rstb.2009.0235.
7. Carreau S, Wolczynski S, Galeraud-Denis I. Aromatase, estrogens and human male reproduction. Philos Trans R Soc Lond B Biol Sci 2010; 365:1571-9; DOI: 10.1098/rstb.2009.0113.
8. Walker WH. Non-classical actions of testosterone and spermatogenesis. Philos Trans R Soc Lond B Biol Sci 2010; 365:1557-69; DOI: 10.1098/rstb.2009.0258.
9. Sharpe RM. Regulation of spermatogenesis. In: The Physiology of Reproduction. Eds. Knobil E, Neill JD. New York, Raven Press 1994; 1363-434.
10. Hess RA. Estrogen in the adult male reproductive tract: A review. Reprod Biol Endocrinol 2003; 1:52; DOI: 10.1186/1477-7827-1-52.
11. Setchell BP. Blood-testis barrier, junctional and transport proteins and spermatogenesis. In: Molecular Mechanisms in Spermatogenesis. Ed. Cheng CY, Austin TX, Landes Bioscience/Springer Science+Business Media, LLC 2008; 212-33.

12. Mruk DD, Silvestrini B, Cheng CY. Anchoring junctions as drug targets: Role in contraceptive development. Pharmacol Rev 2008; 60:146-80; DOI: 10.1124/pr.107.07105.
13. O'Donnell L, Nicholls PK, O'Bryan MK, McLachlan RI, Stanton PG. Spermiation: the process of sperm release. Spermatogenesis 2011; 1:14-35; DOI: 10.4161/spmg.1.1.14525.
14. Parvinen M. Regulation of the seminiferous epithelium. Endocr Rev 1982; 3:404-17; DOI: 10.1210/edrv-3-4-404.
15. Cheng CY, Mruk DD. Regulation of spermiogenesis, spermiation and blood-testis barrier dynamics: novel insights from studies on Eps8 and Arp3. Biochem J 2011; 435:553-62; DOI: 10.1042/BJ20102121.
16. Lie PPY, Mruk DD, Lee WM, Cheng CY. Cytoskeletal dynamics and spermatogenesis. Philos Trans R Soc Lond B Biol Sci 2010; 365:1581-92; DOI: 10.1098/rstb.2009.0261.
17. Vogl AW. Distribution and function of organized concentrations of actin filaments in mammalian spermatogenic cells and Sertoli cells. Int Rev Cytol 1989; 119:1-56; DOI: 10.1016/S0074-7696(08)60648-8.
18. Vogl A, Vaid K, Guttman J. The Sertoli cell cytoskeleton. In: Molecular Mechanisms in Spermatogenesis. Ed. Cheng CY, Austin TX, Landes Bioscience/Springer Science+Business Media, LLC 2008; 186-211.
19. Lie PPY, Mruk DD, Lee WM, Cheng CY. Epidermal growth factor receptor pathway substrate 8 (Eps8) is a novel regulator of cell adhesion and the blood-testis barrier integrity in the seminiferous epithelium. FASEB J 2009; 23:2555-67; DOI: 10.1096/fj.06-070573.
20. Lie PPY, Chan AYN, Mruk DD, Lee WM, Cheng CY. Restricted Arp3 expression in the testis prevents blood-testis barrier disruption during junction restructuring at spermatogenesis. Proc Natl Acad Sci USA 2010; 107:11411-6; DOI: 10.1073/pnas.1001823107.
21. Hayashi K, et al. Domain analysis of the actin-binding and actin-remodeling activities of drebrin. Exp Cell Res 1999; 253:673-80; DOI: 10.1006/excr.1999.4663.
22. Shirao T, et al. Formation of thick, curving bundles of actin by drebrin A expressed in fibroblasts. Exp Cell Res 1994; 215:145-53; DOI: 10.1006/excr.1994.1326.
23. Lappalainen P, Kessels MM, Cope MJ, Drubin DG. The ADF homology (ADF-H) domain: a highly exploited actin-binding module. Mol Biol Cell 1998; 9:1951-9.
24. Shirao T. The roles of microfilament-associated proteins, drebrins, in brain morphogenesis: a review. J Biochem 1995; 117:231-6; DOI: 10.1093/jb/117.2.231.
25. Dun XP, Chilton JK. Control of cell shape and plasticity during development and disease by actin-binding protein Drebrin. Histol Histopathol 2010; 25:533-40.
26. Majoul I, Shirao T, Sekino Y, Duden R. Many faces of drebrin: from building dendritic spines and stabilizing gap junctions to shaping neurite-like cell processes. Histochem Cell Biol 2007; 127:355-61; DOI: 10.1007/s00418-007-0273-y.
27. Peitsch WK, et al. Drebrin is a widespread actin-associating protein enriched at junctional plaques, defining a specific microfilament anchorage system in polar epithelial cells. Eur J Cell Biol 1999; 78:767-78.
28. Keon BH, Jedrzejewski PT, Paul DL, Goodenough DA. Isoform specific expression of the neuronal F-actin binding protein, drebrin, in specialized cells of stomach and kidney epithelia. J Cell Sci 2000; 113:325-36.
29. Grintsevich EE, et al. Mapping of drebrin binding site on F-actin. J Mol Biol 2010; 398:542-54; DOI: 10.1016/j.jmb.2010.03.039.
30. Ishikawa R, et al. Drebrin, a development-associated brain protein from rat embryo, causes the dissociation of tropomyosin from actin filaments. J Biol Chem 1994; 269:29928-33.
31. Kessels MM, Engqvist-Goldstein AE, Drubin DG. Association of mouse actin-binding protein 1 (mAbp1/SH3P7), an Src kinase target, with dynamic regions of the cortical actin cytoskeleton in response to Rac1 activation. Mol Biol Cell 2000; 11:393-412.
32. Sekino Y, Kojima N, Shirao T. Role of actin cytoskeleton in dendritic spine morphogenesis. Neurochem Int 2007; 51:92-104; DOI: 10.1016/j.neuint.2007.04.029.
33. Cheng CY, Mruk DD. An intracellular trafficking pathway in the seminiferous epithelium regulating spermatogenesis: a biochemical and molecular perspective. Crit Rev Biochem Mol Biol 2009; 44:245-63; DOI: 10.1080/10409230903061207.
34. Cheng CY, et al. AF-2364 [1-(2,4-dichlorobenzyl)-1H-indazole-3-carbohydrazide] is a potential male contraceptive: a review of recent data. Contraception 2005; 72:251-61; DOI: 10.1016/j.contraception.2005.03.008.
35. Cheng CY, Mruk DD. New frontiers in non-hormonal male contraception. Contraception 2010; 82:476-82; DOI: 10.1016/j.contraception.2010.03.017.
36. Mok KW, Mruk DD, Lie PPY, Lui WY, Cheng CY. Adjudin, a potential male contraceptive, exerts its effects locally in the seminifeorus epithelium of mammalian testes. Reproduction 2011; 141:571-80; DOI: 10.1530/REP-10-0464.
37. Chen YM, Lee NPY, Mruk DD, Lee WM, Cheng CY. Fer kinase/Fer *T* and adherens junction dynamics in the testis: an in vitro and in vivo study. Biol Reprod 2003; 69:656-72; DOI: 10.1095/biolreprod.103.016881.
38. Li MWM, Mruk DD, Lee WM, Cheng CY. Connexin 43 and plakophilin-2 as a protein complex that regulates blood-testis barrier dynamics. Proc Natl Acad Sci USA 2009; 106:10213-8; DOI: 10.1073/pnas.0901700106.
39. Cheng CY, et al. Two new male contraceptives exert their effects by depleting germ cells prematurely from the testis. Biol Reprod 2001; 65:449-61; DOI: 10.1095/biolreprod65.2.449.
40. Mok KW, Mruk DD, Lee WM, Cheng CY. Spermatogonial stem cells alone are not sufficient to re-initiate spermatogenesis in the rat testis following adjudin-induced infertility. Int J Androl 2011; (In press; DOI: 10.1111/j.1365-2605.2010.01183.x.).
41. Siu MKY, Wong CH, Lee WM, Cheng CY. Sertoli-germ cell anchoring junction dynamics in the testis are regulated by an interplay of lipid and protein kinases. J Biol Chem 2005; 280:25029-47; DOI: 10.1074/jbc.M501049200.
42. Lee NPY, Cheng CY. Regulation of Sertoli cell tight junction dynamics in the rat testis via the nitric oxide synthase/soluble guanylate cyclase/3',5'-cyclic guanosine monophosphate/protein kinase G signaling pathway: an in vitro study. Endocrinology 2003; 144:3114-29; DOI: 10.1210/en.2002-0167.
43. Yan HHN, Mruk DD, Lee WM, Cheng CY. Blood-testis barrier dynamics are regulated by testosterone and cytokines via their differential effects on the kinetics of protein endocytosis and recycling in Sertoli cells. FASEB J 2008; 22:1945-59; DOI: 10.1096/fj.06-070342.
44. Xia W, Wong EWP, Mruk DD, Cheng CY. TGFβ3 and TNFα perturb blood-testis barrier (BTB) dynamics by accelerating the clathrin-mediated endocytosis of integral membrane proteins: A new concept of BTB regulation during spermatogenesis. Dev Biol 2009; 327:48-61; DOI: 10.1016/j.ydbio.2008.11.028.
45. Su L, Mruk DD, Lee WM, Cheng CY. Differential effects of testosterone and TGFβ3 on endocytic vesicle-mediated protein trafficking events at the blood-testis barrier. Exp Cell Res 2010; 316:2945-60; DOI: 10.1016/j.yexcr.2010.07.018.
46. Lui WY, Lee WM, Cheng CY. Transforming growth factor-β3 perturbs the inter-Sertoli tight junction permeability barrier in vitro possibly mediated via its effects on occludin, zonula occludens-1 and claudin-11. Endocrinology 2001; 142:1865-77; DOI: 10.1210/en.142.5.1865.
47. Lui WY, Lee WM, Cheng CY. Transforming growth factor-β3 regulates the dynamics of Sertoli cell tight junctions via the p38 mitogen-activated protein kinase pathway. Biol Reprod 2003; 68:1597-612; DOI: 10.1095/biolreprod.102.011387.
48. Siu MKY, Lee WM, Cheng CY. The interplay of collagen IV, tumor necrosis factor-α, gelatinase B (matrix metalloprotease-9) and tissue inhibitor of metalloprotease-1 in the basal lamina regulates Sertoli cell-tight junction dynamics in the rat testis. Endocrinology 2003; 144:371-87; DOI: 10.1210/en.2002-220786.
49. Butkevich E, et al. Drebrin is a novel connexin-43 binding partner that links gap junctions to the submembrane cytoskeleton. Curr Biol 2004; 14:650-8; DOI: 10.1016/j.cub.2004.03.063.
50. Rottner K, Hanisch J, Campellone KG. WASH, WHAMM and JMY: regulation of Arp2/3 complex and beyond. Trends Cell Biol 2010; 20:650-61; DOI: 10.1016/j.tcb.2010.08.014.
51. Nürnberg A, Kitzing T, Grosse R. Nucleating actin for invasion. Nat Rev Cancer 2011; 11:177-87; DOI: 10.1038/nrc3003.
52. Ahmed S, Goh WI, Bu W. I-BAR domains, IRSp53 and filopodium formation. Semin Cell Dev Biol 2010; 21:350-6; DOI: 10.1016/j.semcdb.2009.11.008.
53. Mruk DD, Cheng CY. The myotubularin family of lipid phosphatases in disease and in spermatogenesis. Biochem J 2010; 433:253-62; DOI: 10.1042/BJ20101267.
54. Li MWM, Mruk DD, Lee WM, Cheng CY. Connexin 43 is critical to maintain the homeostasis of blood-testis barrier via its effects on tight junction reassembly. Proc Natl Acad Sci USA 2010; 107:17998-8003; DOI: 10.1073/pnas.1007047107.
55. Russell LD. Further observations on tubulobulbar complexes formed by late spermatids and Sertoli cells in the rat testis. Anat Rec 1979; 194:213-32; DOI: 10.1002/ar.1091940204.
56. Young JS, Guttman JA, Vaid KS, Vogl AW. Tubulobulbar complexes are intercellular podosome-like structures that internalize intact intercellular junctions during epithelial remodeling events in the rat testis. Biol Reprod 2009; 80:162-74; DOI: 10.1095/biolreprod.108.070623.
57. Young JS, Guttman JA, Vaid KS, Vogl AW. Cortactin (CTTN), N-WASP (WASL) and clathrin (CLTC) are present at podosome-like tubulobulbar complexes in the rat testis. Biol Reprod 2009; 80:153-61; DOI: 10.1095/biolreprod.108.070615.
58. Xia W, Mruk DD, Lee WM, Cheng CY. Cytokines and junction restructuring during spermatogenesis—a lesson to learn from the testis. Cytokine Growth Factor Rev 2005; 16:469-93; DOI: 10.1016/j.cytogfr.2005.05.007.
59. Zhao L, et al. Role of p21-activated kinase pathway defects in the cognitive deficits of Alzheimer disease. Nat Neurosci 2006; 9:234-42; DOI: 10.1038/nn1630.
60. Kojima N, Shirao T. Synaptic dysfunction and disruption of postsynaptic drebrin–actin complex: A study of neurological disorders accompanied by cognitive deficits. Neurosci Res 2007; 58:1-5; DOI: 10.1016/j.neures.2007.02.003.
60a. Siu MKY, Wong CH, Xia W, Mruk DD, Lee WM, Cheng CY. The ß1-integrin-p-FAK-p130Cas-DOCK180-RhoA-vinculin is a novel regulatory protein complex at the apical ectoplasmic specialization in adult rat testes. Spermatogenesis 2011; 1:73-86; DOI: 10.4161/spmg.1.1.15452
61. Lui WY, Wong CH, Mruk DD, Cheng CY. TGFβ3 regulates the blood-testis barrier dynamics via the p38 mitogen activated protein (MAP) kinase pathway: an in vivo study. Endocrinology 2003; 144:1139-42; DOI: 10.1210/en.2002-0211.
62. Lie PPY, Cheng CY, Mruk DD. Interleukin-1α is a regulator of the blood-testis barrier. FASEB J 2011; 25:1244-53; DOI: 10.1096/fj.10-169995.

63. Sarkar O, Mathur PP, Cheng CY, Mruk DD. Interleukin 1alpha (IL1A) is a novel regulator of the blood-testis barrier in the rat. Biol Reprod 2008; 78:445-54; DOI: 10.1095/biolreprod.107.064501.
64. Wong EWP, Mruk DD, Lee WM, Cheng CY. Regulation of blood-testis barrier dynamics by TGFβ3 is a Cdc42-dependent protein trafficking event. Proc Natl Acad Sci USA 2010; 107:11399-404; DOI: 10.1073/pnas.1001077107.
65. Russell L. Movement of spermatocytes from the basal to the adluminal compartment of the rat testis. Am J Anat 1977; 148:313-28; DOI: 10.1002/aja.1001480303.
66. Hess RA, de Franca LR. Spermatogenesis and cycle of the seminiferous epithelium. In: Molecular Mechanisms in Spermatogenesis. Ed. Cheng CY, Austin, TX Landes Bioscience/Springer Science+Business Media, LLC 2008; 1-15.
67. De SK, et al. Expression of tumor necrosis factor-α in mouse spermatogenic cells. Endocrinology 1993; 133:389-96; DOI: 10.1210/en.133.1.389.
68. Mullaney BP, Skinner M. Transforming growth factor-β (β1, β2 and β3) gene expression and action during pubertal development of the seminiferous tubule: potential role at the onset of spermatogenesis. Mol Endocrinol 1993; 7:67-76; DOI: 10.1210/me.7.1.67.
69. Xia W, Mruk DD, Lee WM, Cheng CY. Differential interactions between transforming growth factor-β3/TßR1, TAB1 and CD2AP disrupt blood-testis barrier and Sertoli-germ cell adhesion. J Biol Chem 2006; 281:16799-813; DOI: 10.1074/jbc.M601618200.
70. Goicoechea SM, Arneman D, Otey CA. The role of palladin in actin organization and cell motility. Eur J Cell Biol 2008; 87:517-25; DOI: 10.1016/j.ejcb.2008.01.010.
71. Chin YR, Toker A. Akt2 regulates expression of the actin-bundling protein palladin. FEBS Lett 2010; 584:4769-74; DOI: 10.1016/j.febslet.2010.10.056.
72. Cheng CY, Marther JP, Byer AL, Bardin CW. Identification of hormonally responsive proteins in primary Sertoli cell culture medium by anion-exchange high performance liquid chromatography. Endocrinology 1986; 118:480-8; DOI: 10.1210/endo-118-2-480.
73. Li JCH, Lee WM, Mruk DD, Cheng CY. Regulation of Sertoli cell myotubularin (rMTM) expression by germ cells in vitro. J Androl 2001; 22:266-77.
74. Mruk DD, et al. Role of tissue inhibitor of metalloproteases-1 in junction dynamics in the testis. J Androl 2003; 24:510-23.
75. Galdieri M, Ziparo E, Palombi F, Russo MA, Stefanini M. Pure Sertoli cell cultures: a new model for the study of somatic-germ cell interactions. J Androl 1981; 5:249-59.
76. Li MWM, Mruk DD, Lee WM, Cheng CY. Disruption of the blood-testis barrier integrity by bisphenol A in vitro: Is this a suitable model for studying blood-testis barrier dynamics? Int J Biochem Cell Biol 2009; 41:2302-14; DOI: 10.1016/j.biocel.2009.05.016.
77. Xiao X, Mruk DD, Lee WM, Cheng CY. c-Yes regulates cell adhesion at the blood-testis barrier and the apical ectoplasmic specialization in the seminiferous epithelium of rat testes. Int J Biochem Cell Biol 2011; 43:651-65; DOI: 10.1016/j.biocel.2011.01.008.
78. Lui WY, Cheng CY. Regulation of cell junction dynamics by cytokines in the testis—a molecular and biochemical perspective. Cytokine Growth Factor Rev 2007; 18:299-311; DOI: 10.1016/j.cytogfr.2007.04.009.